Nonradiative processes in the $Zn_{1-x}Co_xSe$ system

Marek Grinberg
Institute of Experimental Physics, University of Gdansk, Wita Stwosza 57, 80-952 Gdansk, Poland

A. C. Felici, T. Papa, and M. Piacentini
Dipartimento di Energetica, Universita di Roma ''La Sapienza,'' Via A. Scarpa 14, 00161 Roma, Italy and Istituto Nazionale di Fisica della Materia, Sezione di Roma I, Roma, Italy

(Received 10 May 1999)

We report the photoacoustic investigations of the $Zn_{1-x}Co_xSe$ system. The qualitative analysis of possible nonradiative deexcitation paths in the Co^{2+} ion is performed. It is shown that the pseudo-Jahn-Teller effect is responsible for accumulation of the electron-lattice interaction energy in the lowest $^2T_1$ state. As a result, the effective path for nonradiative deexcitation of the system is opened. [S0163-1829(99)01736-1]

I. INTRODUCTION

The purpose of this paper is the interpretation of the photoacoustic spectrum of $Zn_{1-x}Co_xSe$ and the qualitative analysis of possible nonradiative deexcitation paths in the Co^{2+} ion.

A Co atom has nine valence electrons in the $3d^7 4s^2$ configuration. When it replaces the Zn^{2+} ions in the zincblende ZnSe lattice, the two *s* electrons are shared with the Se atoms to form tetrahedraly coordinated bonds. The internal energetic structure of the Co^{2+} ion is determined by the remaining seven *d*-electrons, which are influenced by the crystal field of tetrahedral symmetry. The electronic energy levels scheme of the Co^{2+} ion is determined within the framework of the crystal-field theory[1–3] by the values of the Racah parameters B and C, by the crystal-field splitting parameter $10Dq$ and by the spin-orbit interaction parameter ξ.[4] The next parameter that determines the transitions' line shape is the electron-lattice coupling $S\hbar\omega$. According to the spin-selection rules, in the energy region below the ZnSe fundamental energy gap one expects to observe three strong absorption bands related to the spin-allowed transitions from the quartet $^4A_2$ ground state to the quartet $^4T_2$, $^4T_1$(a), and $^4T_1$(b) final states for increasing photon energy. In the case of $^4T_1$ states we have indicated them by a and b instead of the respective atomic quartet states ''F'' and ''P'' since they are completely mixed by the off-diagonal part of the Tanabe-Sugano matrix, equal to $6B$. Many weak absorption bands have been also observed and assigned to final doublet states. The energies of the lowest ^2E, $^2T_1$, and $^2T_2$ doublet states fall between the $^4T_1$(a) and $^4T_1$(b) quartet states. Specifically the $^2T_1$ state, which is just above the $^4T_1$(b) state, can produce significant absorption due to large spin-orbit mixing with the close quartet level.[2]

As far as the luminescence is considered, the IR emission related to the $^4T_2 \rightarrow {}^4A_2$ transition, which accompanies the respective absorption band $^4A_2 \rightarrow {}^4T_2$, can be detected.[5] In the last decade also the emission from the next excited state $^4T_1$(a) has been observed.[6] As far as we know, the emission from higher excited states (^2E and $^2T_1$ doublets or a $^4T_1$(b) quartet), which would be excited only by the $^4A_2 \rightarrow {}^4T_1$(b) absorption band, has not been observed. The sharp lines at 2.36 eV, 2.43 eV, and 2.54 eV, observed in the low-temperature absorption spectra[7,8] and the one at 2.36 eV detected in the emission[8] were attributed to transitions to the states belonging to the mixed (d^7,d^6) electronic configuration.[7]

The electronic energetic structure of the Co^{2+} ion is strongly influenced by the electron-lattice interaction, which is related to the interaction of the ligand ions with the Co^{2+} *d* electrons cloud. In that paper we have considered the coupling of the seven *d* electrons system with the full symmetric a_1 vibrational mode and to the two-dimensional ϵ vibrational mode. We have performed the calculations in the strong crystal-field scheme[4] and the results have been visualized in the form of several configurational coordinate diagrams, which represent separately the electron system coupled to the a_1 mode only, and then to the ϵ mode. In the latter case the calculations also included the Pseudo-Jahn-Teller coupling, which results from coupling between different states of T symmetry via the distortion of the ϵ symmetry. From these configurational coordinate diagrams we have estimated the energy barriers for the nonradiative processes. As a particular, quite fundamental result, we have found that the existence of the Jahn-Teller effect, the Pseudo-Jahn-Teller effect, and the coupling by the B Racah parameter, cause an effective exchange of the Jahn-Teller relaxation energy between the coupled states. It has been found that this effect leads to the accumulation of the lattice relaxation energy in the lowest $^2T_1$ state and, therefore, it reduces significantly the barrier for the nonradiative process between them and the excited state $^4T_1$(a).

In Sec. II we describe the photoacoustic experiment. In Sec. III we discuss the configurational coordinate diagrams. In the Appendix we discuss the analytical result obtained for the simplified case of the $^4T_1$(a) and $^4T_1$(b) states coupled to the ϵ mode.

II. EXPERIMENT

Photoacoustic spectroscopy is a technique, which allows the measurement of absorption coefficients by detection of the heat generated in a sample by the absorption of modulated light. In particular, using a microphone, the acoustic signal generated in a closed cell by the periodic heat flow from a solid sample to the surrounding gas can be measured. With respect to other conventional techniques, the photoacoustic spectroscopy presents some advantages as, for example, the possibility of changing the optical density of the sample without any destructive preparation, simply varying the chopping frequency of the absorbed light. Since the photoacoustic signal is related only to that fraction of absorbed energy which is converted into heat photoacoustic spectroscopy, provides information on nonradiative deexcitation processes.

According to the Rosengwaig and Gersho theory,[9] in the case of thermally thick solids (the thermal diffusion length μ_s is shorter than the sample thickness), the photoacoustic signal is approximately proportional to the absorption coefficient α if the condition $\alpha^{-1} > \mu_s$ is satisfied. When $\alpha^{-1} < \mu_s$ the signal becomes independent of the sample optical response and the photoacoustic spectra show saturation.

Our experimental set up[10,11] consisted of a 500-W Xe lamp coupled with a $f/4$ Jobin-Yvon monochromator and a mechanically chopped at 20 Hz photoacoustic cell with Bruel and Kjaer microphone detector, a lock-in amplifier, and a computer-controlled acquisition system. The experiments were performed at room temperature and the energy range from 0.6 eV to 3.0 eV was covered with an energy resolution of about 20 meV. In order to eliminate the contribution from the spectral response of the optical apparatus, the photoacoustic signal measured for the sample was divided by the photoacoustic signal measured for a completely absorbing material such as graphite. Each spectrum was normalized to the saturation value. Single crystals of $Zn_{1-x}Co_xSe$ were grown by the chemical transport method with I_2 as a carrier medium. The transition metal concentrations $x = 0.001$ and $x = 0.015$ were determined by means of x-ray fluorescence spectroscopy.

III. CALCULATIONS AND DISCUSSION

To obtain the energy structure of our system we have considered the Hamiltonian

$$H_{tot} = H_{cf} + H_{s\text{-}o} + H_{latt} + H_{e\text{-}latt}, \qquad (1)$$

where H_{cf} and $H_{s\text{-}o}$ are the electronic parts of the Hamiltonian describing the crystal-field and the spin-orbit interactions, respectively. H_{latt} is the lattice potential energy and $H_{e\text{-}latt}$ is the electron-lattice interaction. The crystal field and the spin-orbit parts of the Hamiltonian have been valuated by the Racah parameters, B and C, the crystal-field parameter, $10Dq$, and the spin-orbit parameter ξ. We have used the same set of values for these parameters as those used by Uba and Baranowski.[2] Thus, $10Dq = 3500\ \text{cm}^{-1}$, $B = 590\ \text{cm}^{-1}$, $C = 1970\ \text{cm}^{-1}$, and the spin-orbit interaction parameter $\xi = 375\ \text{cm}^{-1}$. The energetic structure of the system has been obtained by means of the Tanabe-Sugano matrix calculated in the strong field approximation[4] and the spin-orbit interaction Hamiltonian derived by Runciman and Schroder.[12] We have represented four possible electronic configurations of the $3d^7$ electrons in the tetrahedral crystal field by the 120 -$|SLJM\rangle$ orbitals.[13]

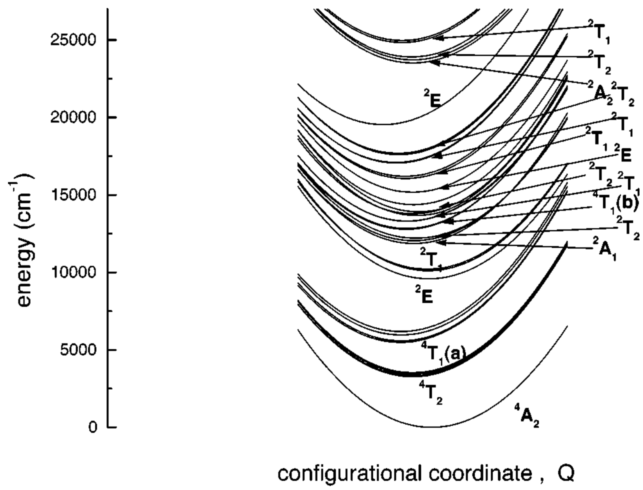

FIG. 1. Configurational coordinate diagram of the Co^{2+} ion in ZnSe describing the system coupled to the full symmetrical a_1 mode. Parameters of the diagram are given in the text.

The lattice Hamiltonian, H_{latt}, has been considered in the harmonic approximation as a potential proportional to the sum of the squares of the symmetrized displacements of the ions. The electron-lattice interaction, $H_{e\text{-}latt}$, was taken into account in the linear approximation. The electron lattice coupling was defined by the lattice relaxation energy, E_{rel}. For the coupling to the breathing mode, E_{rel} is related to $S\hbar\omega$, where S is the Huang-Rhys parameter and $\hbar\omega$ is the phonon energy. In the case of coupling with the ϵ mode E_{rel} was related to the Jahn-Teller stabilization energy $E_{J\text{-}T}$. As presented further, we can consider the interaction with different modes separately without any loss in generality.

A. Coupling to the a_1 mode

In the case of coupling to the breathing mode, the matrix elements of the electron-phonon interaction have been considered as the diagonal part of the Hamiltonian in the form

$$H_{e\text{-}latt} = n\sqrt{2S\hbar\omega}Q, \qquad (2)$$

where Q is the configurational coordinate and n depends on the electronic configuration according to the formula $e^{4-n}t^{3+n}$. Since the ground state $^4A_2$ belongs to the electronic configuration e^4t^3 and the first excited state belongs to the electronic configuration e^3t^4, $S\hbar\omega$ can be estimated from the experimental value of the lattice relaxation energy of the first excited state $^4T_2$. In our calculations we used $S\hbar\omega = 130\ \text{cm}^{-1}$, following the value suggested by Radlinski,[5] for the electron-lattice coupling energy in the $^4T_2$ state (e^3t^4 electronic configuration). The details concerning the derivation of the one-dimensional configurational coordinate diagrams are presented elsewhere.[14] The one-dimensional configuration coordinate diagram for the Co^{2+} is presented in Fig. 1. We present here only the states with energies below $30\,000\ \text{cm}^{-1}$.

As far as the ZnSe:Co system is considered both theoretical calculations[15] and the experimental photoconductivity measurements[7] yield the energy of the ground state of the Co^{2+} ion about 2.3 eV below the bottom of the conduction band (d^6 and an electron in the conduction band). Therefore, it is not necessary to take into account the influence of the conduction band; the transitions below this energy are analyzed. Thus, one can consider the d^7 configurational coordinate diagram presented in Fig. 1 as a good approximation of the energetic structure of the system.

Let us focus on the calculation of the radiative transition probabilities resulting from this diagram. To get the diagram presented in Fig. 1 we have diagonalized the Hamiltonian, which is in the form of a 39×39 matrix with the spin-orbit interaction that mixes the states of different spins. Thus, each electronic manifold in the diagram is represented by the electronic wave function given by the linear combination of the doublet (indicated as ${}^2\varphi$) and quartet (indicated as ${}^4\varphi$) components,[16]

$$\phi_\nu(q,Q)=\sum_n a_{\nu m}^{(4)}(Q)^4\varphi_m(q)+\sum_n a_{\nu n}^{(2)}(Q)^2\varphi_n(q). \tag{3}$$

The sets of coefficients $a_{\nu m}^{(4)}$ and $a_{\nu n}^{(2)}$ obtained from the diagonalization represent the contributions of the quartet-mth and doublet-nth orbitals to the final ν state. In Eq. (3) q represents the electronic coordinate and Q represents the ionic coordinate, respectively.

To relate the energy of the absorption line to the respective final-state electronic manifold we considered the vertical Frank-Condon transitions that correspond to the maxima of the absorption bands. Since the initial state for the absorption is the ground electronic manifold with the minimum for $Q=0$, these transitions take place for $Q=0$. Since the contributions of doublet states to the ground state are negligible, the transition probability of each absorption line is approximately proportional to the following sum:

$$P_\nu=\sum_m |a_{\nu m}^{(4)}(Q=0)|^2. \tag{4}$$

Note that under such assumption we get the same histograms representing the transition probabilities for any vibrational mode with which the system is coupled.

In order to obtain the real absorption, one has to relate the specific band shape (Gaussian, Pekarian, or any other) to each transition . One expects to reproduce the real line shape by consideration of phonon repetitions resulting from coupling to different symmetry modes. However, we do not analyze our experimental spectra in this way since they do not contain enough details. The main purpose of calculations presented here is the analysis of possible contributions of the higher excited doublet states to the absorption bands. The results of our calculations, presented as vertical bars, whose lengths are proportional to the transition probabilities, are compared with the experimental photoacoustic spectra in Fig. 2. We have obtained good coincidence between the two strong photoacoustic peaks and the calculated probabilities of the ${}^4A_2\rightarrow{}^4T_1$(a) and ${}^4A_2\rightarrow{}^4T_1$(b) transitions. The energy of the ${}^4A_2\rightarrow{}^4T_2$ transition falls below the lowest photon energy available in our experiment. Also, the doublet states close to the ${}^4T_1$(b) state, i.e., the ${}^2T_1$ and ${}^2T_2$ states above it and the doublets ${}^2A_1$ and ${}^2T_2$ just below it, contribute to the absorption spectrum. Actually, the tails near the absorption band ${}^4A_2\rightarrow{}^4T_1$(b) (see Fig. 2) in the photoacoustic spectra can be attributed to borrowing the oscillator strength from the central quartet state. One has to notice that our calculations of the radiative transition probabilities are in agreement with the results obtained by Klein *et al.*[17] for Co in ZnS and ZnSe.

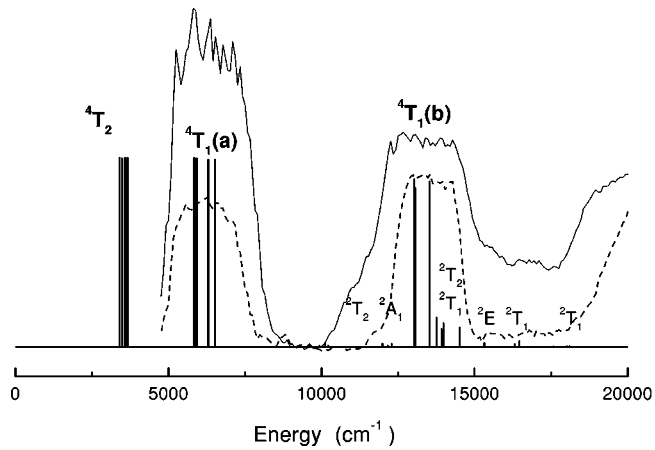

FIG. 2. The reproduced absorption and photoacoustic signal intensity related to the Co^{2+} ion in ZnSe. Calculated transition probabilities are represented by the vertical lines. Curves correspond to the photoacoustic spectra of $Zn_{1-x}Co_xSe$ for $x=0.015$ (solid curve) and $x=0.001$ (dashed curve).

As far as the nonradiative relaxation processes are considered we have assumed that they are related mainly to the internal conversion transitions for which the kinetics and selection rules have been described by Grinberg and Mandelis.[18,19] In general, the internal conversion between two electronic manifolds can take place if they are close enough and mixed by the specific interaction. In our case, this mixing occurs mainly due to the spin-orbit interaction.

Even a short glance at the diagram in Fig. 1 allows us to predict that the system excited to the ${}^4T_1$(b) state very easily relaxes nonradiatively to the lower ${}^2A_1$ and ${}^2T_2$ electronic manifolds, which are very close in energy and strongly coupled by the spin-orbit interaction with the ${}^4T_1$(b) state. It seems that also further nonradiative relaxation to the ${}^2T_1$ and ${}^2E$ states is quite probable. The nonradiative transitions from the ${}^2E$ state to the lower ${}^4T_1$(a) state are much less probable. Therefore, there is no serious reason not to expect the existence of the radiative transitions from the ${}^2E$ state. Although the radiative ${}^2E\rightarrow{}^4A_2$ transition is spin-forbidden, the nonradiative internal conversion to the ${}^4T_1$(a) state seems to be still not effective enough to quench it. One can see from the diagram in Fig. 1 that the ${}^4T_1$(a) manifold is at the same (or even smaller) distance from the ${}^4T_2$ electronic manifold as ${}^2E$ from ${}^4T_1$(a). Additionally, the states of the same spin are mixed by the spin-orbit and electron-phonon interactions, whereas the states of different spins are mixed only by the spin-orbit interaction. The spin-selection rule holds for the optical as well as for the internal-conversion transitions. For this reason the nonradiative process between the states with the same spin $[{}^4T_1(\mathrm{a})-{}^4T_2]$ should be more probable than between a doublet and a quartet state $[{}^2E$ and ${}^4T_1(\mathrm{a})]$. As a consequence, the ratio of the radiative to nonradiative rate should be approximately the same for the $[{}^2E-{}^4T_1(\mathrm{a})]$ and $[{}^4T_1(a)-{}^4T_2]$ electronic manifolds. Contrary to this fact, only the luminescence from the ${}^4T_1$(a) state and not that from the higher ^2E state has been observed. We have to conclude that the approximation of considering only the coupling to the full symmetrical lattice mode cannot explain this discrepancy.

B. Coupling to the ϵ mode. Jahn-Teller and pseudo-Jahn-Teller effects

To take into account the coupling to the ϵ mode one has to consider the electron-lattice interaction Hamiltonian,

$$H_{e\text{-}latt}(Q_u,Q_v)=\frac{\partial V}{\partial Q_u}Q_u+\frac{\partial V}{\partial Q_v}Q_v, \tag{5}$$

where Q_u and Q_v are the normal coordinates representing the two-dimensional mode of ϵ symmetry.

As mentioned above, we have used a basis of 120 $|\mathrm{SLJM}\rangle$ states. Actually due to the Kramer degeneration this number has been reduced to 60. The matrix elements of electron-lattice Hamiltonian (5) have been calculated using the Clebsch-Gordon coefficients tabulated by Koster *et al.*[20] for thirty two point groups. To get all possible couplings we have followed the same scheme as that used by Uba and Baranowski[2] for the case of $(^4T_1,{}^4T_1)*\epsilon$ Jahn-Teller coupling. According to the group theory, only the T_1,T_2 states, and separately the E states, the E with A_1 states, and the E with A_2 states, are coupled via the ϵ mode. In general, one should introduce different coupling constants for each pair of states mentioned above. For sake of simplicity we have assumed that all states of T symmetry are coupled by the same constant, related to the $(T_1,T_1)*\epsilon$ Jahn-Teller stabilization energy by the relation

$$V=\sqrt{2E_{J-T}}, \tag{6}$$

independently if we deal with T_1-T_1, T_1-T_2, or T_2-T_2 pairs. The states of E symmetry and the E and A pairs have been assumed to be not affected by the ϵ lattice mode; thus, the respective coupling constants have been assumed to be equal to zero. Such an assumption is mainly related to the fact that, for Co^{2+} in ZnSe, the value of the electron-lattice coupling can be derived only for the T states from the analysis of the absorption and emission bands. Thus any value we could use for the $E*\epsilon$ coupling is completely arbitrary. The value zero is as good as any other. Since most of the states have either T_1 or T_2 symmetry, we believe that most of the phenomena related to nonradiative processes can be described by considering only the T states. Even if our estimation of the electron-lattice coupling in the E states is wrong, it does not influence much our final results. To be in coincidence with calculations performed for coupling to the breathing mode and also with the calculations performed by Uba and Baranowski,[2] we have assumed that the Jahn-Teller stabilization energy is 425 cm^{-1}.

In order to show how particular interactions influence the configuration coordinate diagram we performed the calculations taking only account of the Jahn-Teller effect, and then we included the pseudo-Jahn-Teller coupling between the different states of T symmetry. In both cases the spin-orbit interaction was at first neglected and then taken into account.

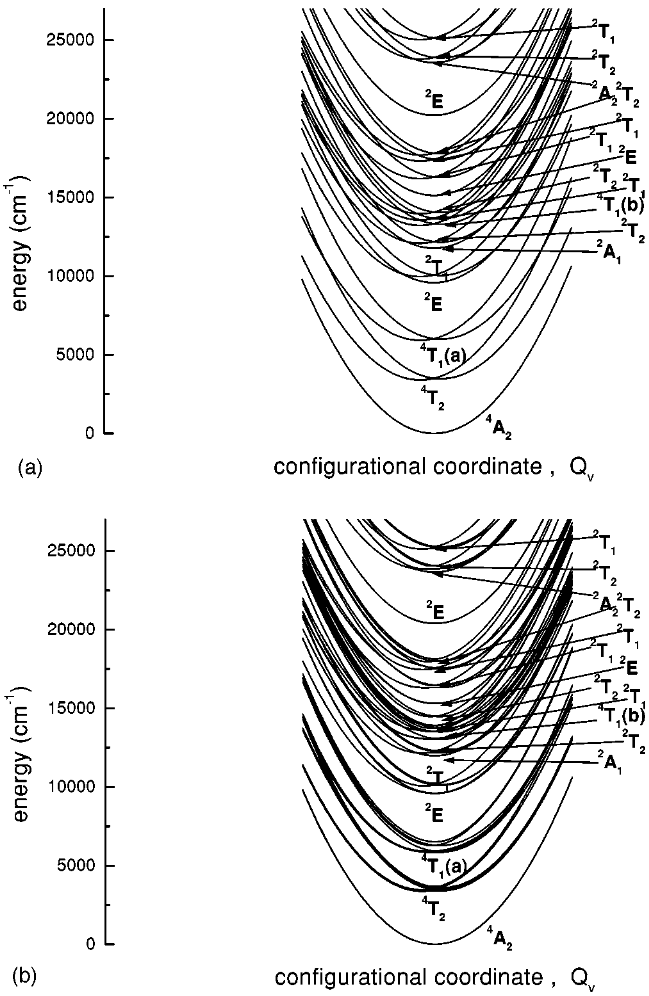

FIG. 3. Configurational coordinate diagram of the energetic structure of tetrahedrally coordinated Co^{2+}, which includes the Jahn-Teller $T*\epsilon$ effect. The calculations, which omit and include the spin-orbit interaction are presented in panels (a) and (b), respectively. In the diagrams the cross sections along the Q_v axis are presented.

To take into account only the Jahn-Teller effect we considered the quasidiagonal Hamiltonian that includes only the matrix elements of the electron-lattice coupling of individual quartets and doublets. All matrix elements that couple the components of different states are ignored. The results of these calculations are presented in Figs. 3(a) and 3(b), respectively. In both figures we show the cross section of the potential-energy sheets along the Q_v axis. One can notice that the shape and the splitting at $Q_v=0$ of the adiabatic potential energies of the second excited term, $^4T_1$(a), are different from those obtained by Uba and Baranowski.[2] This difference can be explained considering that we have taken into account the 120 components of all possible states of the d^7 electronic configuration instead of 12 components corresponding to the $^4T_1(F)$ state only as done by Uba and Baranowski.[2] In fact, the $^4T_1$ state cannot be related to a particular ionic quartet, F or P, since they are completely mixed by the strong interaction represented by the matrix element equal to $6B$.[4]

As far as the nonradiative processes are considered, one can see that since we assumed the medium electron-lattice coupling constant (the same for each state) we still cannot

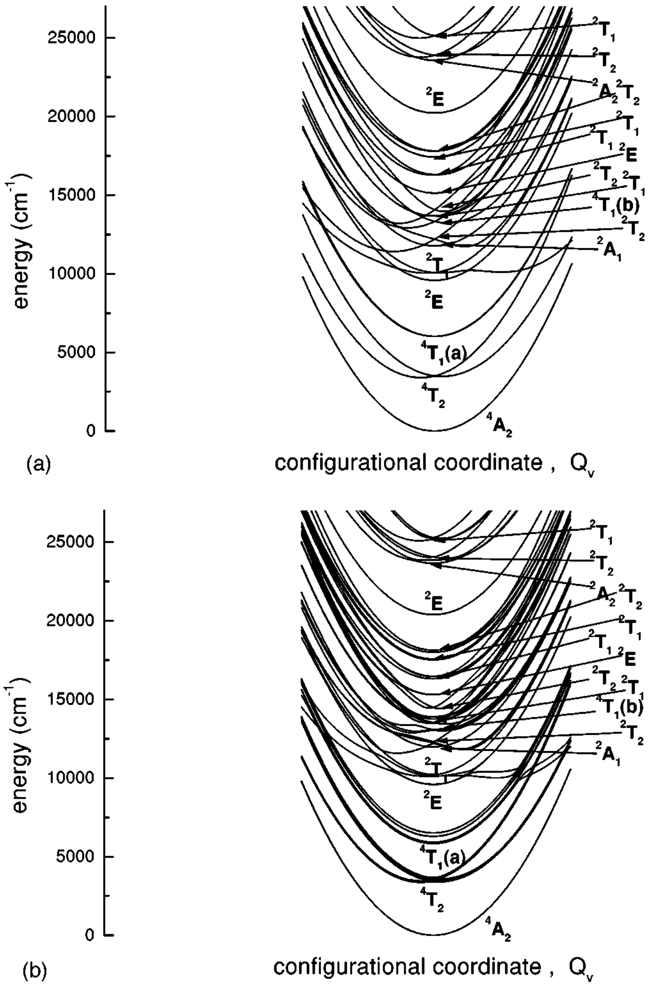

FIG. 4. Configurational coordinate diagram of the energetic structure of tetrahedrally coordinated Co^{2+}, which includes the Jahn-Teller $T*\epsilon$ effect and the pseudo-Jahn-Teller $T*\epsilon$ effect. The calculations, which omit and include the spin-orbit interaction, are presented in panels (a) and (b), respectively. In the diagrams, the cross-sections along the Q_v axis are presented.

evidence the effective path for nonradiative relaxation to the lower electronic manifolds, which can explain the lack of emission from the ^2E state.

The situation changes dramatically when the Pseudo-Jahn-Teller effect is considered. In Figs. 4(a) and 4(b) the respective configuration coordinate diagrams are presented without and with the spin-orbit interaction, respectively. To get these diagrams we have considered the full electron-lattice coupling Hamiltonian that includes the coupling between different electronic manifolds. The picture is clearer when Fig. 4(a) is considered. One can see that, with respect to Fig. 3(a), the structure of splitting does not change, but the large quantitative changes as far as the quantity of the splitting in different states take place.

Considering the similarities and differences between the diagrams presented in Fig. 3 a as well as Fig. 4(b) and Figs. 4(a) and 4(b) one can notice that the structure and the quantity of splitting of the $^4T_2$ state did not change. This is expected, since this state is not coupled with other states by the Racah parameters. A more complicated situation occurs in the case of the $^4T_1$(a) and $^4T_1$(b) states. Here the amount of splitting of the $^4T_1$(a) state is almost negligible, whereas the amount of splitting of the $^4T_1$(b) state is much larger than in the case when the Pseudo-Jahn-Teller effect is neglected. In the case of the $^2T_1$ and $^2T_2$ states the changes are even more dramatic. All splitting cumulates in the lowest $^2T_1$ and $^2T_2$ states, whereas the higher excited states are less splitted. Actually, the last effect is responsible for a significant decrease of the barrier for nonradiative processes between the $^2T_1$ and $^4T_1$(a) states [see Figs. 4(a) and 4(b)]. Therefore, the probability of nonradiative processes in the ^2E and $^2T_1$ doublets has to be quite large and certainly quenches the luminescence. Although the effect of accumulation of the electron-lattice interaction energy in the particular states seems to be queer it is a simple consequence of superposition of the interstates electron-lattice coupling (the Pseudo-Jahn-Teller effect) and electrostatic interaction given by the Racach matrix *B*. To present this phenomena in a clearer way we considered separately the simplest case of coupling between $^4T_1$(a) and $^4T_1$(b) states in the Appendix.

IV. CONCLUSIONS

We have discussed the electron-lattice coupling on the electronic structure and radiative and nonradiative processes in Co^{2+} in ZnSe. We have explained the lack of ^2E-$^4A_2$ emission by strong decrease of the energy barrier for nonradiative transitions due to the accumulation of the electron-lattice relaxation energy in the $^2T_1$ state. It has been shown that this effect is caused by the strong pseudo-Jahn-Teller coupling in the number of $^2T_1$ and $^2T_2$ states. It is known that the pseudo-Jahn-Teller effect changes the curvature of the adiabatic potentials in the upper and in the lower mixed states. An example, that concerns however only the pseudo-Jahn-Teller interaction without Jahn-Teller splitting has been given by Opik and Pryce[21] for the system of two states accidentally degenerated. The case presented in this paper is in fact an extension of the Opik and Pryce example. The main difference is that we have taken into account both the pseudo-Jahn-Teller and the standard Jahn-Teller effect. Considering the Tanabe-Sugano matrices for any system, one can see that the situation like that presented for $^4T_1$(a) and $^4T_1$(b) is rather typical.[4] Often, one has the relative small values of the diagonal Hamiltonian and large values of the off-diagonal matrix elements (of the order of a few *B* or even a few *C* Racah parameters). This overlook leads to a quite general conclusion concerning the predictions of the strength of Jahn-Teller effects in the transition-metal complexes. It is very probable that pseudo-Jahn-Teller coupling, usually not considered for these systems, is in fact very important. It can be one of the reasons that, although the crystal-field approximation seems to work quite good (even quantitatively) as far as the energetic structure is considered, it almost never provides a good prediction for the strength of the electron-lattice coupling.

ACKNOWLEDGMENTS

This paper was supported in part by the Polish Committee for Scientific Research, Grant No. 2P03B003 13. One of us (M.G.) acknowledges the University of Rome ''La Sapienza'' for a two-month stay as Visiting Professor.

APPENDIX

It is interesting to investigate a phenomena of exchange of the Jahn-Teller relaxation energy in more detail. It is relatively easy to consider the $^4T_1(\mathrm{a})$ and $^4T_1(\mathrm{b})$ pairs. The electron-lattice coupling and the crystal-field Hamiltonian for this system can be represented by the following 6×6 matrix:

$$\begin{matrix} \alpha Q_v \\ 0 & \beta Q_v \\ 0 & 0 & \beta Q_v \\ 6B+\alpha Q_v & 0 & 0 & E+\alpha Q_v \\ 0 & 6B+\beta Q_v & 0 & 0 & E+\beta Q_v \\ 0 & 0 & 6B+\beta Q_v & 0 & 0 & E+\beta Q_v, \end{matrix} \tag{A1}$$

where $\alpha=V$ and $\beta=-0.5V$,[22] $E=10Dq-9B$, where B is the Racah parameter. In our representation the diagonal matrix elements correspond to the electronic (crystal-field) energy and the Jahn-Teller energy, whereas the off-diagonal matrix elements correspond to the pseudo-Jahn-Teller coupling. One can reduce the problem of 6×6 matrix to three 2×2 matrices. The splitting resulting from the Jahn-Teller effect in the absence of the $^4T_1(\mathrm{a})$ and $^4T_1(\mathrm{b})$ mixing is given by

$$\Delta_0=(\alpha-\beta)Q_v, \tag{A2}$$

and is the same in both the $^4T_1(\mathrm{a})$ lower and the $^4T_1(\mathrm{b})$ upper state. When the mixing is included, one obtains following splittings:

$$\Delta_u=\Delta_0+\Delta \tag{A3}$$

and

$$\Delta_l=\Delta_0-\Delta, \tag{A4}$$

for upper and lower state, respectively, where

$$\Delta=0.5[\sqrt{E^2+4(6B+\alpha Q_v)^2}-\sqrt{E^2+4(6B+\beta Q_v)^2}] \tag{A5}$$

One can neglect the E energy in comparison to $6B$. Thus, for reasonable Q_v one obtains

$$\Delta=(\alpha-\beta)Q_v. \tag{A6}$$

Considering relations (A2)–(A6), one can easily see why the splitting almost disappears in the $^4T_1(\mathrm{a})$ state, whereas the splitting of the $^4T_1(\mathrm{b})$ state increases about two times. The same effect takes place for the doublet states. However, here the situation is more complicated since for both the $^2T_1$ and $^2T_2$ states the pseudo-Jahn-Teller matrix is 5×5.

One should point out that we have a different situation in the case of the pseudo-Jahn-Teller in the $^4T_2$,$^4T_1$ states that are not coupled by any Tanabe-Sugano matrix and the initial splitting between them is $11B$ or $10Dq+3B$ depending on which state the $^4T_1(\mathrm{a})$ or $^4T_1(\mathrm{b})$ is considered. In this case, additional splitting induced by the pseudo-Jahn-Teller effect is

$$\Delta=1/E(\alpha^2-\beta^2)Q_v^2, \tag{A7}$$

which is small compared to the Jahn-Teller splitting, Δ_0

[1] E. M. Wray and J. W. Allen, J. Phys. C **4**, 512 (1971).
[2] S. M. Uba and J. M. Baranowski, Phys. Rev. B **17**, 69 (1978).
[3] A. P. Radlinski, Phys. Status Solidi B **84**, 503 (1977).
[4] S. Sugano, Y. Tanabe, and H. Kamimura, *Multiplets of Transition Metal Ions in Crystals* (Academic, New York, 1970).
[5] A. P. Radlinski, J. Lumin. **18/19**, 147 (1979).
[6] G. Goetz and H-J. Schulz, Phys. Status Solidi B **169**, 217 (1992).
[7] J. M. Noras, H. R. Szawelska, and J. W. Allen, J. Phys. C **14**, 3255 (1981).
[8] D. J. Robbins, P. J. Dean, J. L. Glasper, and S. G. Bishop, Solid State Commun. **38**, 61 (1980).
[9] A. Rosencwaig and A. Gersho, J. Appl. Phys. **47**, 64 (1976).
[10] A. C. Felici, N. Galbato, D. Debowska, T. Papa, M. Piacentini, and F. Lama, Nuovo Cimento A **16**, 163 (1994).
[11] A. C. Felici, F. Lama, M. Piacentini, T. Papa, D. Debowska, A. Kisiel, and A. Rodzik, J. Appl. Phys. **80**, 6925 (1996).
[12] W. A. Runciman and K. A. Schroeder, Proc. R. Soc. London, Ser. A **265**, 489 (1962).
[13] B. G. Wybourne, *Spectroscopic Properties of Rare Earth* (Interscience, New York, 1965).
[14] Cz. Koepke, K. Wisniewski, M. Grinberg, D. L. Russel, K. Holloday, and G. H. Beall, J. Lumin. **78**, 135 (1998).
[15] A. Fazzio, M. J. Caldas, and Alex Zunger, Phys. Rev. B **30**, 3430 (1984).
[16] M. Grinberg, J. Lumin. **54**, 369 (1993).
[17] K. Klein, J. Dreyhsig, H.-E. Gumlich, M. Thiede, G. Goetz, H.-J. Shulz, and J. W. Allen, Phys. Status Solidi A **130**, K207 (1992).
[18] M. Grinberg, A. Mandelis, and K. Fieldsted, Phys. Rev. B **48**, 5923 (1993).

[19] M. Grinberg and A. Mandelis, Phys. Rev. B **49**, 12 496 (1994).
[20] G. F. Koster, J. O. Dimmock, R. G. Wheler, and H. Statz, *Properties of Thirty Two-Point Groups* (MIT, Cambridge, MA, 1963).
[21] U. Opik and M. H. L. Pryce, Proc. R. Soc. London, Ser. A **238**, 425 (1957).
[22] R. Englman, *Jahn-Teller Effect in Molecules and Crystals* (Wiley, New York, 1972).